Inductively Coupled Plasma Source Using Internal Multiple U-Type Antenna for Ultra Large-Area Plasma Processing

Jong Hyeuk Lim, Kyong Nam Kim, Geun Young Yeom*

An inductively coupled plasma source with internal-type linear inductive antennas named as "internal multiple U-type antenna" was developed for the substrate size of $2\,300 \times 2\,000$ mm^2 and the characteristics of the large-area inductive plasma source were investigated. High density plasmas on the order of 1.18×10^{11} cm^{-3} could be obtained at the pressure of 15 mTorr Ar gas and the RF power of 8 kW with good plasma stability. In addition, by using variable capacitors at the end of the antenna, lower antenna voltage and more uniform antenna voltage distribution could be obtained. When a photoresist film was etched using O_2 plasma with 8 kW RF power, an etch uniformity less than 11% could be obtained using the multiple U-type antenna on the substrate size larger than 7th generation ($2\,200 \times 1\,870$ mm^2).

Introduction

Inductively coupled plasma (ICP) sources have been widely investigated as effective tools for microelectronic device processing. In addition, due to their geometric simplicity and ability to produce uniform high density plasma, the ICP sources have been also widely investigated for the large-area plasma processing applied to flat panel displays (FPDs) among the high-density plasma sources such as ICP,[1–3] electron cyclotron resonance (ECR) plasma,[4] helicon plasma,[5] etc.

For FPDs, as the substrate size increases, due to the extremely large size of the substrate, obtaining high plasma uniformity at high plasma density over the substrate area becomes more important. Currently, as the conventional antenna for ICP sources, external spiral-type antennas located on the top of the dielectric window are generally used to obtain uniform and high-density plasmas. However, as the processing area is increased, conventional ICPs having the external spiral antenna show some problems such as a large voltage on

the antenna, and the increased thickness of dielectric window, etc.[6] When a large voltage is induced on the spiral antenna, capacitive coupling to the plasma with a low power transfer efficiency and unstable impedance matching results. In addition, the increase in the dielectric window thickness causes the deterioration of the power transfer efficiency from the antenna to the plasma in addition to the increase in manufacturing cost.[1,6] Also, the long antenna length can exhibit a standing wave effect which results in unstable and non-uniform plasmas.[3,7] To reduce the standing wave effect with increasing antenna length, various configurations of the internal-type antenna having low impedances have been investigated by a few researchers.[8–10]

In this work, we present an internal-type ICP source that enables large-area ($2\,300 \times 2\,000$ mm^2) plasma generation. As the internal-type antenna, a multiple U-type antenna array, where the antenna was composed of four pairs of single U-type antenna connected in parallel, was used and its electrical characteristics and the plasma characteristics were investigated to study the possibility of overcoming standing wave effect and large antenna voltage on the antenna. In some cases, for the uniform distribution of current to each U-type antenna, variable capacitors were connected and their effects on the plasma characteristics were also investigated.

J. H. Lim, K. N. Kim, G. Y. Yeom
Department of Materials Science and Engineering, Sungkyunkwan University, Suwon, Kyunggi-do, 440-746, South Korea
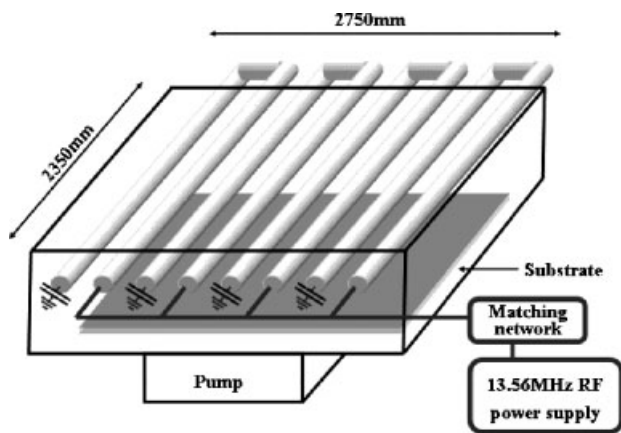E-mail: gyyeom@skku.edu

WILEY
InterScience®
DISCOVER SOMETHING GREAT

Figure 1. Schematic diagram of the ICP system with multiple U-type antenna used in the experiment.

Experimental Part

The experimental setup of the internal ICP system used in this study is schematically shown in Figure 1. The processing chamber has a rectangular shape with the size of $2\,750 \times 2\,350$ mm^2 for the application of large-area FPD processing and the substrate size was $2\,300 \times 2\,000$ mm^2 (larger than 7th generation substrate: $2\,200 \times 1\,870$ mm^2). As shown in Figure 1, the multiple U-type antenna consisted of four pairs of U-type antennas connected in parallel and one side of the antenna was connected to a 10 kW 13.56 MHz RF power generator through an L-type matching network while the other side was connected to ground directly or to ground through a variable capacitor. The distance between antennas was 320 mm and the distance between the antenna and the chamber wall was 160 mm. The antenna was made of 25.5-mm-diameter copper tubing for water cooling and the outside of the antenna was coaxially covered by quartz tubing with an outer diameter of 33 mm and a thickness of 1.5 mm.

To investigate the characteristics of the plasmas, a Langmuir probe (Hiden Analytical Inc., ESP) was installed at 19 cm below the antenna and at the center of the chamber (total height of the processing chamber: 650 mm). The electrical properties of the internal antenna were measured by an impedance analyzer (MKS Inc.) located between the matching box and the antenna. In addition, each U-type antenna voltage was measured using a high voltage probe (Textronix 6015A). For an estimation of plasma uniformity, a 2-μm thick photoresist film coated glass covering the substrate area of $2\,200 \times 2\,000$ mm^2 was placed on the substrate and its etch depth was measured. The photoresist etch depth was measured using a step profilometer (Tencor Inc., Alpha-step 500).

Results and Discussion

Figure 2 shows the characteristics of the plasma measured at the center of the chamber as a function of RF power at 15 mTorr of Ar for the antennas connected to ground directly (grounded antenna) and the antennas connected to ground through a variable capacitor (floated antenna).

Figure 2(a) shows the plasma density measured using a Langmuir probe as a function of RF power for the grounded antenna and the floated antenna. As shown in the figure, as the RF power is increased from 1 to 8 kW, the plasma density is increased almost linearly for both the grounded antenna and the floated antenna. However, the floated antenna shows a little higher plasma density compared to the grounded antenna and, at 8 kW RF power, a high-density plasma of about 1.18×10^{11} cm^{-3} could be obtained for the floated antenna.

Figure 2(b) shows the plasma potential and electron temperature of the plasmas measured for the condition shown in Figure 2(a). As shown in the figure, the plasma potential is generally decreased with the increase in RF power for both the grounded antenna and the floated antenna, and the grounded antenna shows a higher plasma potential compared to the floated antenna at a given power. The increase in RF power also decreases the electron temperature for both antennas as shown in the figure and the floated antenna also shows a lower electron temperature compared to the grounded antenna. For 8 kW of RF power and 15 mTorr Ar, the grounded antenna shows the plasma potential of about 36 V and the electron temperature of about 2.96 eV while the floated antenna shows the plasma potential of about 28 V and the electron temperature of about 2.89 eV. The decrease in plasma potential and electron temperature with increasing RF power is believed to be related to the increase in inductive coupling to the plasma compared to capacitive coupling and, the increase in plasma density with the increase in RF power shown in Figure 2(a) is also believed to be related not only to the increase in power input to the plasma but also to the increase in inductive coupling by the antenna to the plasma. The lower plasma potential and the lower electron temperature shown for the floated antenna compared to those for the grounded antenna decrease possible contamination to the substrate by decreasing the energy of the charged particle to the chamber wall, electrodes, etc.

Figure 3(a) shows the RF RMS voltage and current measured using an impedance probe for both antennas as a function of RF power at 15 mTorr Ar. As shown in the figure, the RF RMS voltage increases with the increase in RF power for both antennas and the grounded antenna shows higher RF antenna voltage compared to the grounded antenna. High RF RMS voltage on the antenna can increase the dc voltage induced on the quartz tubing covering the antenna and can increase the sputtering of the dielectric material of the tubing which increases the particles and contamination to the substrate in addition to the unstable plasma characteristics.[11–14] The effect of the reduced rms rf coil voltage on the decrease of quartz tube sputtering is confirmed by measuring the dc potential shift on the insulator covering the antenna. The RF coil voltage V_a and
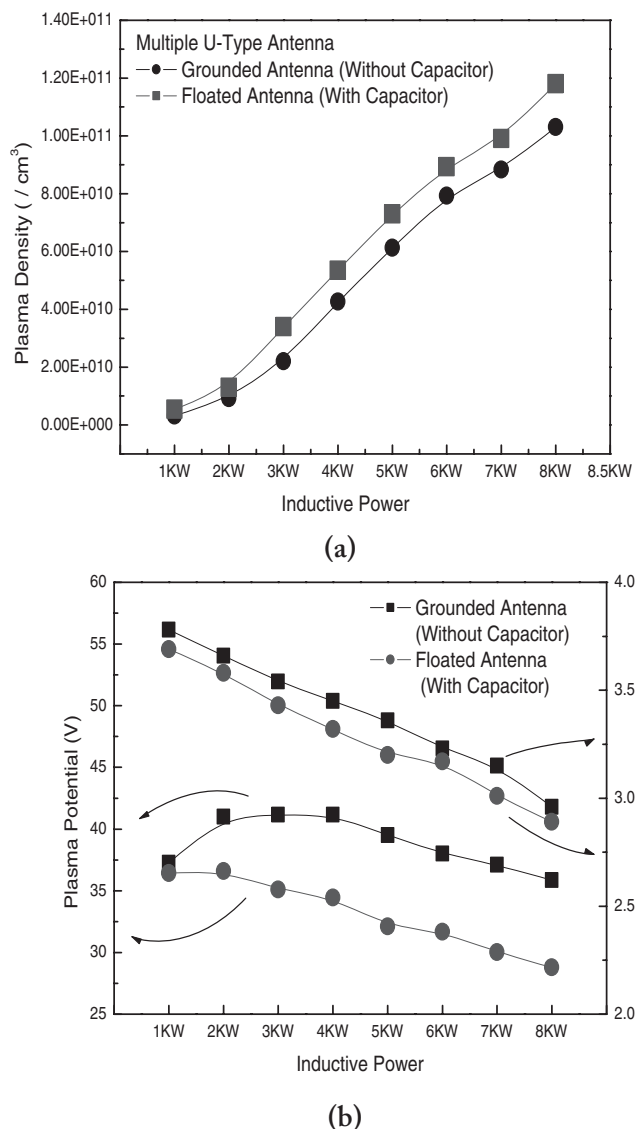
Inductively Coupled Plasma Source Using Internal Multiple U-Type Antenna . . .

Plasma Processes
and Polymers

(a)

(b)

Figure 2. (a) Ar$^+$ ion density measured by a Langmuir probe at 19 cm below the antenna as a function of RF power for the grounded antenna and the floated antenna. (b) Plasma potential and electron temperature calculated as a function of RF power for both antennas. RF input power to the antennas was varied from 1 to 8 kW and the operation pressure was maintained at 15 mTorr of Ar.

the RF voltage of the insulator covering the antenna conductor V_s, which is proportional to the DC bias voltage V_{DC} on the insulator, were related by the following simple equation in the internal linear ICP[15,16]

$$V_{DC} \propto Vs \cong \frac{C_i}{C_i + C_s} V_a \qquad (1)$$

where C_i is the capacitance between the antenna and the quartz surface and C_s the capacitance between the quartz surface and the plasma. From this equation, it is clarified

that the electrostatic coupling which results in quartz tube sputter etching is strongly dependent on the rms coil voltage V_a and the distance between the antenna and quartz tube. Therefore, the use of floated antenna appears to show a more stable and clean plasma compared to the grounded antenna. In the case of RF RMS current, as shown in Figure 3(b), the increase in RF power increases the RF RMS current rapidly up to 4 kW and further increase in RF power appears to increase the current slowly or saturate the current gradually for both antennas. When the currents of both antennas are compared, the grounded antenna shows a lower RF RMS current at a fixed RF power. The change in current increase with increase of RF power at about 4 kW appears to be related to the change in antenna coupling from capacitive coupling to inductive coupling. Also, the higher RF RMS current and the lower RF RMS voltage shown for the floated antenna appear to show more inductive coupling compared to the grounded antenna as indicated by higher plasma density in Figure 2(a).

Figure 3(b) shows the power transfer efficiency calculated for the floated antenna in Figure 3(a). The power transfer efficiency was calculated from the relationship among the input power to the antenna, the RF RMS current, and the resistance:[6,17,18] $\left(\frac{\text{Input power} - I_{RF}^2 R}{\text{Input power}} \times 100\right)$. Here, $I_{RF}^2 R$ $(P_{\text{Joule loss}} = I_{RF}^2 R)$ is the Joule loss due to the current flowing in the antenna. The power transfer efficiency was also calculated by the relationship among the RF RMS voltage, RF RMS current, and the phase difference between the voltage and current $(V_{rms} I_{rms} \cos\theta)$ measured at the location between the matching network and the antenna, and the difference between the two methods was less than 5%. As shown in the figure, the power transfer efficiency increased with the increase in RF power and, at 8 kW of RF power, the power transfer efficiency of about 83% was obtained.

Figure 4(a) and 4(b) show the RF RMS voltage measured for 5 kW of RF power and for 15 mTorr O$_2$ at each U-type antenna input location along the chamber wall using a high voltage probe for the grounded and floated antennas, respectively. As shown in Figure 4(a), the antenna input voltage measured along the chamber wall is not uniform for each U-type antenna of the grounded type possibly due to the difficulty in maintaining the same antenna length for four U-type antennas from the power input to ground. By adding a variable capacitor between the ground and each U-type antenna line and, by varying the capacitance from 300 to 400 pF, relatively uniform voltage distribution on each antenna as shown in Figure 4(b) can be obtained. Also, as shown in Figure 4(b), by adding the capacitor, lower antenna voltages are obtained on each antenna for the floated type. The more uniform and lower antenna voltage
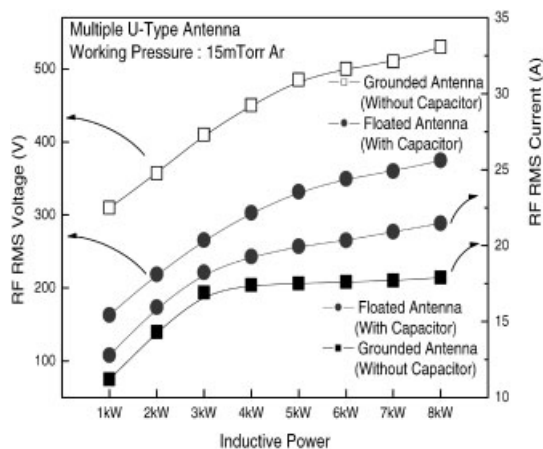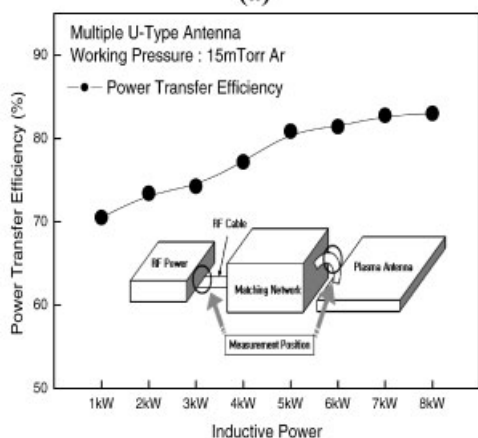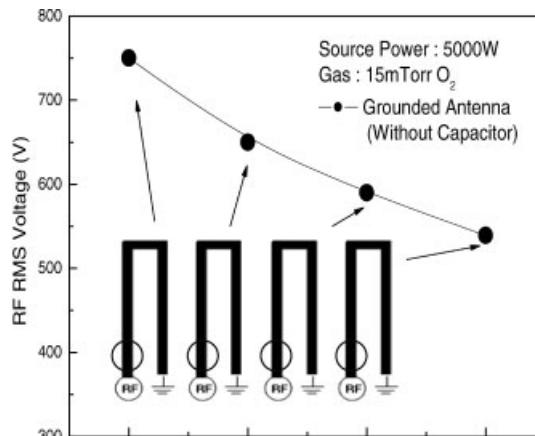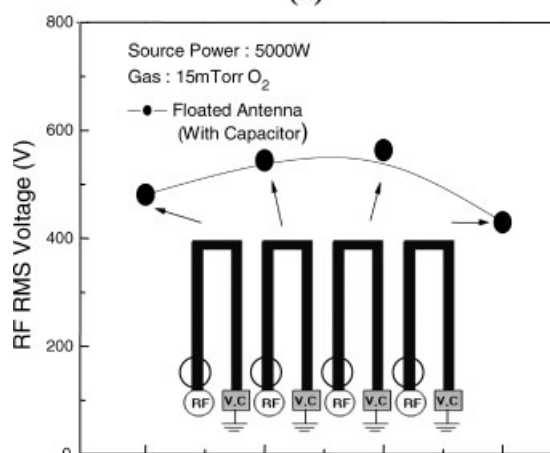
Figure 3. (a) RF RMS voltage and current of the internal-type ICP measured by an impedance analyzer on the antenna located close to the RF power input for the grounded antenna and the floated antenna. (b) Power transfer efficiency for the floated antenna measured by an impedance analyzer as function of RF power. 15 mTorr of Ar was used and the RF power was varied from 1 to 8 kW.

Figure 4. RF RMS voltage on the multiple U-type antenna measured by a high voltage probe at an inductive power of 5 kW and an O_2 pressure of 15 mTorr for the grounded antenna (a) and for the floated antenna (b).

obtained by the floated antenna is believed to be related to the formation of uniform impedance for each antenna.

When the grounded antenna is used, due to the non-uniform voltage of the antenna across the chamber, non-uniform plasma across the processing chamber could be estimated by etching the photoresist covering the substrate area (not shown). However, by using the floated antenna, more uniform plasma across the chamber could be estimated. Figure 5 shows the photoresist etch uniformity measured by etching the photoresist for the floated antenna at 5 kW RF power and 15 mTorr O_2 gas using 2-μm thick photoresist coated glass covering the substrate area of $2\,300 \times 2\,000$ mm². The etch uniformity of the photoresist film was acheived with O_2 gas due to the high photoresist etch rate compared to Ar gas and the operation with O_2 gas did not show significant differences compared to that with Ar gas. As shown in the figure, using

the floated antenna, about 11% of etch uniformity, and possibly a plasma density of about 11% could be obtained on a substrate size of $2\,300 \times 2\,000$ mm².

Conclusion

In this study, as an application to the plasma processing of large-area FPD (substrate size of $2\,300 \times 2\,000$ mm²: larger than 7th generation glass), an internal-type antenna composed of multiple U-type antennas was used as the ICP source and the electrical characteristics of the antenna and the plasma characteristics were investigated. Also, by connecting a variable capacitor in the range of 300–400 pF at the end of each U-type antenna line, the effect of the capacitor on the electrical characteristics of the antenna and the plasma characteristics were compared. The results
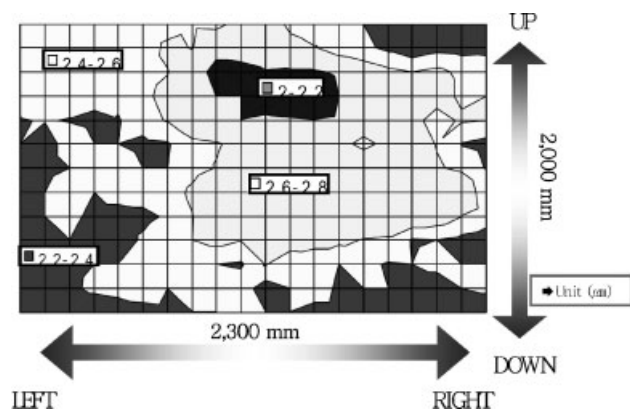
Inductively Coupled Plasma Source Using Internal Multiple U-Type Antenna . . .

Plasma Processes
and Polymers

Figure 5. Etch uniformity (in μm) of the photoresist film on the substrate area of 2 300 $\times$ 2 000 mm^2 measured at 5 kW RF power and 15 mTorr O$_2$.

showed that, by connecting the capacitor to the antenna (floated antenna), lower RF RMS antenna voltage, higher RF RMS antenna current, and higher power transfer efficiency could be obtained resulting in higher plasma density, lower plasma potential, and lower electron temperature of the plasma. By using the floated antenna, at 8 kW of RF power and 15 mTorr Ar, a plasma density of about 1.07×10^{11} cm^{-3} could be obtained at 19 cm below the antenna and at the center of the chamber. The capacitance of the capacitors connected at the end of the U-type antenna needs to be optimized to obtain uniform antenna voltage along the chamber wall, and, when the photoresist was etched using 15 mTorr O$_2$ and at 5 kW of RF power after the optimization of capacitance of the capacitor, about 11% etch uniformity of photoresist could be obtained over the substrate area of 2 300 $\times$ 2 000 mm^2.

[1] T. Meziani, P. Colpo, F. Rossi, *Plasma Source Sci. Technol.* **2001**, *10*, 276.
[2] M. Kanoh, K. Suzuki, J. Tonotani, K. Aoki, M. Yamage, *Jpn. J. Appl. Phys.* **2001**, *40*, 5419.
[3] Y. Wu, M. A. Liberman, *Appl. Phys. Lett.* **1998**, *72*, 777.
[4] S. Matsuo, Y. Adachi, *Jpn. J. Appl. Phys.* **1982**, *21*, 4.
[5] J. E. Stevens, M. J. Sowa, J. L. Cecchi, *J. Vac. Sci. Technol.* **1995**, *A13*, 5.
[6] J. Hopwood, *Plasma Source Sci. Technol.* **1994**, *3*, 460.
[7] K. N. Kim, S. J. Jung, G. Y. Yeom, *J. Appl. Phys.* **2005**, *97*, 063302.
[8] Y. Setuhara, T. Shoji, A. Ebe, S. Baba, N. Yamamoto, K. Takahashi, K. Ono, S. Miyake, *Surf. Coat. Technol.* **2003**, *33*, 174.
[9] K. Suzuki, K. Konishi, K. Nakamura, H. Sugai, *Plasma Source Sci. Technol.* **2000**, *9*, 199.
[10] K. N. Kim, Y. J. Lee, S. J. Kyong, G. Y. Yeom, *Surf. Coat. Technol.* **2004**, *752*, 177.
[11] Y. J. Lee, K. N. Kim, G. Y. Yeom, *Appl. Phys. Lett.* **2004**, *85*, 1677.
[12] Y. Setuhara, S. Miyake, Y. Sakawa, T. Shoj, *Jpn. J. Appl. Phys.* **1999**, *38*, 4263.
[13] F. Heinrich, U. Banziger, A. Jentzsch, G. Neumann, C. Huth, *J. Vac. Sci. Technol.* **1996**, *B14*, 2000.
[14] K. N. Kim, M. S. Kim, G. Y. Yeom, *Appl. Phys. Lett.* **2006**, *88*, 161503.
[15] H. Sugai, K. Nakamura, K. Suzuki, *Jpn. J. Appl. Phys.*, **1994**, *33*, 2189.
[16] Y. Wu, M. A. Lieberman, *Plasma Sources Sci. Technol.* **2000**, *9*, 210.
[17] R. B. Piejak, V. A. Godyak, B. M. Alexandrovich, *Plasma Source Sci. Technol.* **1992**, *1*, 179.
[18] M. Kanoh, K. Suzuki, J. Tonotani, K. Aoki, M. Yamage, *Jpn. J. Appl. Phys.* **2001**, *40*, 5419.